Angle resolved photoemission spectroscopy (ARPES)

Gautam Aditya Kavuri (10976)

1 Green's functions

The theory of photo-emission is most easily studied with the help of Green's functions. Following the example of [1], we define the causal one-particle Green's function as follows, and do a spectral decomposition:

$$\begin{aligned}
G(k,\tau) =& -i\langle \mathbf{T}\hat{c}_k^\dagger(\tau)\hat{c}_k(0)\rangle \\
=& -i\Theta(-\tau)\langle N|e^{-i\hat{H}\tau}c_k e^{i\hat{H}\tau}c_k^\dagger|N\rangle \\
&+ i\Theta(+\tau)\langle N|c_k^\dagger e^{-i\hat{H}\tau}c_k e^{i\hat{H}\tau}|N\rangle \\
=& -i\Theta(-\tau)\sum_m \langle N|e^{-i\hat{H}\tau}c_k|N+1,m\rangle\langle N+1,m|e^{i\hat{H}\tau}c_k^\dagger|N\rangle \\
&+ i\Theta(+\tau)\sum_i \langle N|c_k^\dagger e^{-i\hat{H}\tau}|N-1,i\rangle\langle N-1,i|c_k e^{i\hat{H}\tau}|N\rangle \\
=& -i\Theta(-\tau)\sum_m e^{-i(E_n-E_m)\tau}|\langle N+1,m|c_k^\dagger|N\rangle|^2 \\
&+ i\Theta(+\tau)\sum_i e^{+i(E_n-E_i)\tau}|\langle N-1,i|c_k|N\rangle|^2
\end{aligned} \tag{1}$$

Next, we do an (incomplete) Fourier transform, by multiplying by $e^{i(\omega\tau\pm i\delta)}$, as appropriate, where we introduce the small positive quantity δ. We then obtain the result in [1]:

$$G^\pm(k,\omega) = \sum_m \frac{|\langle N\pm1,m|c_k^\pm|N\rangle|^2}{\omega - E_m^{N\pm1} + E^N \pm i\delta} \tag{2}$$

Next, we use the integral identity obtained by integrating around a semi-circular contour on the complex plane , $\int_{-\infty}^{\infty}\frac{1}{x\pm i\delta}dx = P(\int_{-\infty}^{\infty}(1/x)) \mp i\pi$, and define the so called spectral function as $A(k,w) = (1/\pi)Im(G(k,w))$. Clearly then:

$$A^\pm(k,w) = \sum_m |\langle N\pm1,m|c_k^\pm|N\rangle|^2\delta(\omega - E_m^{N\pm1} + E_i^N) \tag{3}$$

Where $A(k,\omega) = A^+(k,\omega) + A^-(k,\omega)$. The full Green's function, $G^-(k,\omega) + G^+(k,\omega)$, can be written as (at $T = 0$, noninteracting):

$$G(k,\omega) = \frac{1}{\omega - E_k + \mathrm{sgn}(E_k - E_{k_F})i\delta} \tag{4}$$

From 4, , one can see at once the*Lehmann representation* of the Green's function:

$$G(k,w) = \int_{-\infty}^{\infty} \frac{d\omega'}{2\pi} \frac{A(k,\omega')}{\omega - \omega' + \mathrm{sgn}(\omega' - E_{k_F})i\delta} \tag{5}$$

Now, notice that the total Green's function, which is the sum of two terms in 2, has poles on the complex plane as given by the figure, seperated from the real axis by a distance δ.

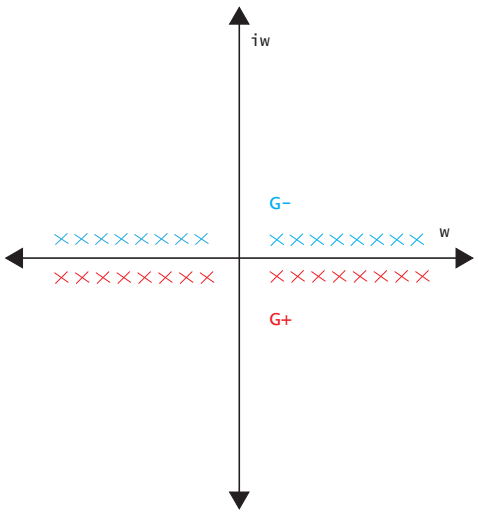

Figure 1: Poles of advanced and retarded Green's functions.

In the limit of $\delta \to 0$, we can rewrite 5 as [4]:

$$G(k,\omega) = \int_{-\infty}^{\infty} \frac{d\omega' A(k,\omega')}{2\pi(\omega - \omega')} \tag{6}$$

Now, consider:

$$\begin{aligned}\lim_{\delta\to 0^+}[G(k,w+i\delta)-G(k,\omega-i\delta)] &= \lim_{\delta\to 0^+} -i\int_{-\infty}^{\infty}\frac{d\omega' A(k,\omega')\delta}{\pi((\omega-\omega')+\delta^2)} \\ &= -i\int_{-\infty}^{\infty}\lim_{\delta\to 0^+}\frac{\delta}{\pi((\omega-\omega')+\delta^2)}d\omega' A(k,\omega') \\ &= -i\int_{-\infty}^{\infty}\delta(\omega-\omega')d\omega' A(k,\omega') \\ &= -iA(k,\omega)\end{aligned} \tag{7}$$

Note that the Green's function given by 6 has divergences along the real line at all points where $A(k,\omega)\neq 0$

2 Equipment and uncertainty

The first step in conducting ARPES is the generation of the X-ray radiation that provides photons for the emission of electron. The X-rays are typically produced by an "undulator", which consists of a series of magnets in an array as shown in 2. The x-rays are mostly produced at the points of maximum curvature on the free electron path. Radiation from an undulator such as this can be tuned over a wide range of frequencies.

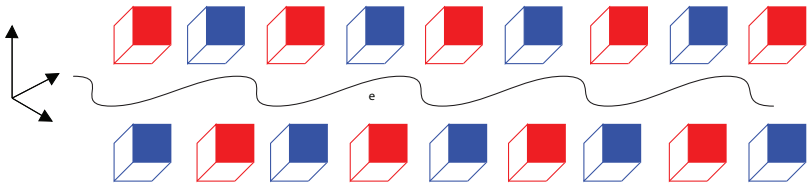

Figure 2: A schematic of an undulator x-ray source.

The radiation is then frequency selected and shaped before it is impinged on a thin slice of the sample in question. The electron then travels through an electrostatic lens before being fed into a hemispherical analyzer. This device consists of two concentric hemispheres of radii (r_1, r_2) maintained at different potentials, say (V_1, V_2), as shown in fig 3. Then, the potential in the space between the hemispheres is given by, using $V_1 - V_2 = Q(1/r_1 - 1/r_2)$, $V(r) = -[\Delta V r_2 r_1/((r_2 - r_1)r)]$. Then, writing down the equations for motion, the effective potential equation in r is:

$$V_{eff}(r) = \frac{l^2}{2mr^2} - eEr \tag{8}$$

using $\frac{l^2}{2mr^2} = E_o$, we obtain the following condition for an electron path that maintains a constant radius [1]:

$$E_o = \frac{e\Delta V}{\frac{r_1}{r_2} - \frac{r_2}{r_1}} \tag{9}$$

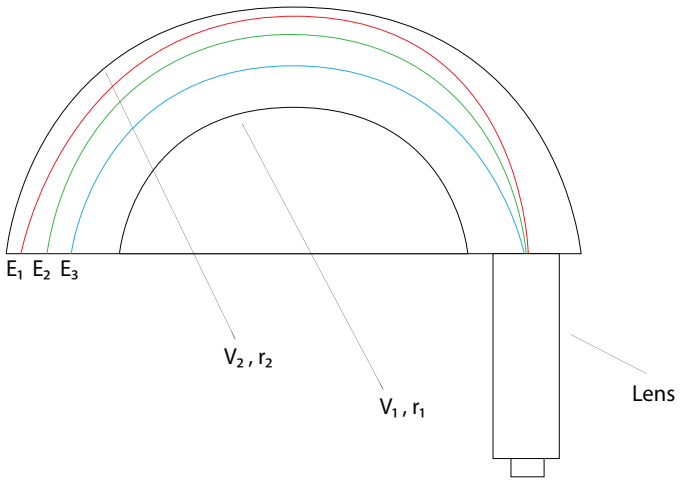

Figure 3: A hemispherical analyzer

Due to the finite thickness of the exit aperture, a small range of energies are allowed through. Further, one can show that the dispersion of the electrons in space is linear in energy, to the first order [2]:

$$\delta r_{exit} = -\delta r_{enter} - 2\alpha^2 r_o + \frac{2\Delta E r_o}{E_o} \tag{10}$$

Here, α is the angle of input electron wrt vertical (assumed to be small). From this, we can read off the uncertainty in the determination of the electron energy [1]:

$$\Delta E = E_o(\frac{w}{2r_o} - \frac{\alpha^2 E_o}{4}) \tag{11}$$

Improving resolution means increasing r_o, which is limited by physical constraints, decreasing E_o, which lowers the reading level and introduces noise and jitter, or decreasing w, which cannot be decreased beyond diffraction limits. In practice, the resolutions are around $2meV$ for $20eV$ photon incident on sample [1]. To conduct an energy scan, usually the hemispheres are held at fixed potentials, and the electrostatic lens, shown in 3 is used to reduce or increase the energy of the photo-electrons to the optimum value E_o. Note that there can be significant uncertainty introduced due to the photon monochromator, which comes after the undulator, also.

Now, in an actual ARPES measurement, the sample is bombarded with photons and the resulting energy of the emitted photoelectrons is measured at

various angles by moving the analyzer. One usually ignores the contribution from photon momentum, and writes down the equation for the kinetic energy of the electrons as [1]:

$$E_{kin} = h\nu - \phi - E_b \tag{12}$$

Where ϕ is the work function that gives the difference between the fermi and vaccum energies, E_b is the binding energy, which is measured wrt the fermi surface. (please refer fig. 4 directly reproduced from [1])

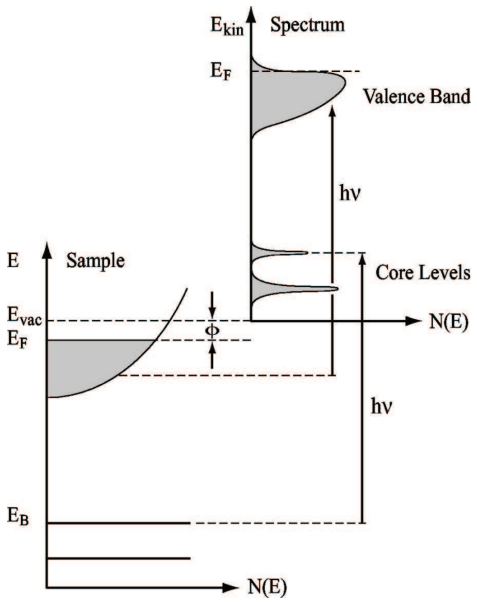

Figure 4: A diagram illustrating various photoemission energies. Graph to the right illustrates the energy scales of the detected free electron. From Hüfner 1995

Now, with the knowledge of the energy, measured experimentally, we can write down the equation for the fermi wave-vector of the electron inside the material, modulo a reciprocal lattice vector, assuming the parallel component of the momentum is conserved across the surface:

$$p_{\parallel e^-} = \hbar k_{\parallel} = \sqrt{2mE_{kin}} sin\theta \tag{13}$$

Here, θ is the angle from the normal to the surface of the sample. Note that the perpendicular component of the momentum is not conserved across the surface, hence we must treat it differently. One way to do this is introduce a potential V_o that takes care of these effects, and write (this simple approximation does not always work [3]):

$$p_{\perp e^-} = \sqrt{2m(E + V_o) - \hbar^2 k_{\parallel}^2} \tag{14}$$

Finally, by varying θ and $h\nu$, one can, probe the variation in energy with $k_{\|}$ and $k_{\perp}$, and thus , probe different values of $k_{\|}$, and thus reconstruct the electronic dispersion $E(\mathbf{k})$ in the material. Note that the uncertainty in $\mathbf{k}$ arises from both the uncertainty in the measurement of angle, and the uncertainty in $E_k in$.

3 Mechanism

The mechanism of photoemission can be explained via a "three-step approximation". We follow closely here the arguments in [1]. The three steps involved are:

1. Excitation of the electron.
2. Diffusion of electron to surface.
3. escape of the electron.

For the first step, we have initially the ground state wave function Ψ_i^N. Upon excitation, we get the excited N-electron wave function Ψ_f^N. Next, we seek to factor out the photo-electron wave function from the final state, as that is what is experimentally detected. In order to simplify this task, we invoke the *sudden approximation*, which basically means that the photo-electron is removed so quickly from the ground state that there is no time for the electron to interact and affect the state of the system left behind. Then we write [1]:

$$\Psi_f^N = \mathbf{A}\phi_f^k \Psi_f^{N-1} \tag{15}$$

Here, Ψ_f^{N-1} is the $N-1$ particle eigenstate of the system in question. Next, we consider the initial state, and following [1], assume that the N body wavefunction can be written as a slater determinant. Then, we can factorize out the single electron wavefunction, by definition:

$$\Psi_i^N = \mathbf{A}\phi_i^k \Psi_i^{N-1} \tag{16}$$

Next, to estimate the contribution of step one in the three step process, we use the fermi golden rule to calculate the transition from the state Ψ_i^N to the state Ψ_f^N under the periodic harmonic perturbation of the photon. The rate is given by:

$$w_{i\to f} = \frac{2\pi}{\hbar}|\langle\Psi_f^N|H_{int}|\Psi_i^N\rangle|^2\delta(E_f^N - E_i^N - h\nu) \tag{17}$$

Under the dipole approximation, we can write the H_{int} as: $\frac{-e}{mc}\mathbf{A}\cdot\mathbf{p}$.
The matrix element in the rate equation is:

$$M_{f,i}^k = \langle\Psi_f^N|H_{int}|\Psi_i^N\rangle = \langle|\phi_f^k|H_{int}|\phi_i^k\rangle\langle\Psi_m^{N-1}|\Psi_i^{N-1}\rangle \tag{18}$$

Where Ψ_f^{N-1} has been replaced by the eigenstate Ψ_m^{N-1}.

Finally, we get the result that that:

$$I(k,w) \propto |M_{f,i}^{k}|^2 \sum_{m} |cm,i|^2 \delta(E_{kin} + E_m^{N-1} - E_i^N - h\nu) \tag{19}$$

Where $c_{m,i} = \langle \Psi_m^{N-1} | \Psi_i^{N-1} \rangle$. Note that this matrix element is not always 1 or 0. In a strongly interacting system, for example, the $N-1$ final state with one electron missing will have a different Hamiltonian, and its eigenstate will differ from the slater combination of $N-1$ orbitals in an N electron system. In the non-interacting limit, only one of these terms survives, and we are left with a perfect delta looking spectrum (ignoring broadening effects from electron diffusion to surface). Thus, precisely speaking, we will get other multiplicative factors from steps 2 and 3 of the three step photoemission process. Also, the matrix element $|M_{f,i}^{k}|^2$ can be shown to depend on the symmetry of the probed state, for instance.

4 Measurement and experiment

Now, comparing with eq 3, we can write eq 19 as [1]:

$$I(k,w) \propto I_o(k,\nu,\mathbf{A}) f(\omega) A^{-}(k,\omega) \tag{20}$$

Where $I_o \propto |M_{f,i}^{k}|^2$ and a finite temperature effect has been introduced by adding $f(\omega)$. We thus arrive at the important result that the measured intensity of photoemission electron is directly related to the *electron removal spectral function* $A^{-}(\cdots)$. This result establishes ARPES as an effective probe of the underlying physics of different materials.

As mentioned earlier, we get a delta function spectral function for a non-interacting system. In real systems, though, one observes a broad peak, and not a delta-like behaviour for $A^{-}(k,\omega)$. We can show that this broadening can be interpreted as the excitations of *quasiparticles*, as detailed in the Landau fermi liquid theory. To see this, first consider a Lorentz-broadened spectrum peaked at ϵ_k given by [4]:

$$A(k,\omega) = A_b(k,\omega) + \frac{2|\gamma_k| w_k}{(\omega - \epsilon_k) + \gamma_k^2} \tag{21}$$

Here, the $A_b(k,\omega)$ is an incoherent background, and γ_k is the width of the peak at ϵ_k, while w_k is the *weight* of the peak [1]. As γ_k and A_b tend to zero, we recover the non-interacting limit.

Now, we use a result that can be proved without too much effort using the operator definition of the Green's functions (zero temperature):

$$\langle n(k) \rangle = \langle a_k^{\dagger} a_k \rangle = \int_{-\infty}^{\infty} \frac{d\omega A(k,\omega)\theta(\omega)}{2\pi} \tag{22}$$

Using this, one can show:

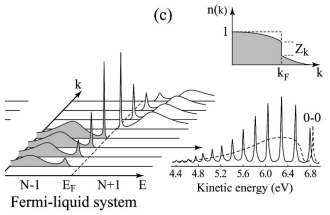

Figure 5: A figure depicting the shape of the electron and hole excitation spectra for a normal Fermi liquid, showing the background and the peak. From Damascelli (2003)

$$\begin{aligned}\langle n(k_F^-)\rangle - \langle n(k_F^+)\rangle =& \frac{2|\gamma_k|\omega_{k_F}}{2\pi}\int_{-\infty}^{\mu}\frac{d\omega}{(\omega-\epsilon_{k_F^+})^2+\gamma_{k_F^+}^2} - \\ & \frac{2|\gamma_k|\omega_{k_F}}{2\pi}\int_{-\infty}^{\mu}\frac{d\omega}{(\omega-\epsilon_{k_F^-})^2+\gamma_{k_F^-}^2} \\ =& \lim_{k\to k_F}\frac{2w_{k_F}}{\pi}\tan^{-1}\left(\frac{|\epsilon_k-\mu|}{|\gamma_k|}\right)\end{aligned} \tag{23}$$

The quantity in the brackets can be shown to be zero for a class of *normal* systems [4], so we obtain the result that the discontinuity in electron occupation at the fermi surface is equal to the weight of the quasi-particle peak at the fermi surface.

However, more interestingly, it is found that many high temperature superconductors do not follow the fermi liquid behaviour even at temperatures higher than T_C, i.e., in the *normal state*. This is especially true of cuprate superconductors [1].

The characteristic of a BCS superconductor is the opening up of a superconducting energy gap, Δ_{SC} below the critical temperature. in *conventional* superconductors, the gap is isotropic. The gap arises, roughly, because $2\Delta_{SC}$ is the energy required to break apart a cooper pair. In *unconventional* superconductors, however, the gap has the symmetry of a $d_{x^2-y^2}$ orbital [5]. ARPES studies can give insight into this, as they can probe the momentum dependance, and make it possible to measure the width of the gap also. For example consider fig 5, here, the midpoint of the excitation spectrum shifts back below T_C, indicating the formation of a forbidden region. Also, the intensity is a product

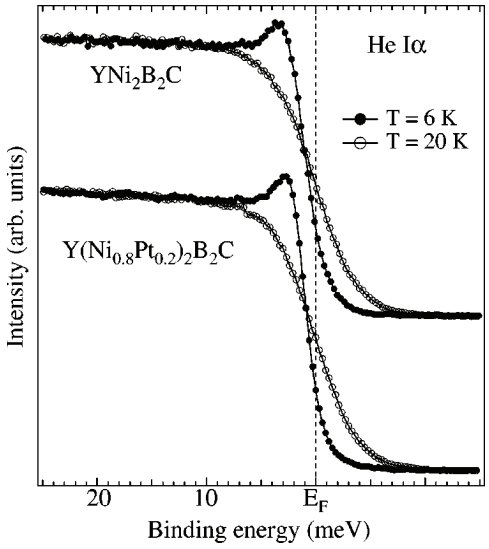

Figure 6: The quasiparticle excitation plots below and above T_C for 2 superconductors. From SAmascelli (2003)

of density of states and the spectral function at non-zero temperatures, so the small peak in the angle averaged intensity serves to indicate a piling up of the density of states. This is, of course, only barely scratching the surface of what can be done using ARPES, and it stands today as one of the most effective and direct tools to probe electronic properties, and goes hand in hand with many of the latest theoretical developments in the field of condensed matter.

References

[1] Damascelli, Andrea, Zahid Hussain, and Zhi-Xun Shen. "Angle-resolved photoemission studies of the cuprate superconductors." Reviews of modern physics 75, no. 2 (2003): 473.

[2] Hadjarab, F., and J. L. Erskine. "Image properties of the hemispherical analyzer applied to multichannel energy detection." Journal of electron spectroscopy and related phenomena 36, no. 3 (1985): 227-243.

[3] Lynch, David W., and Clifford G. Olson. "Photoemission Studies of High-Temperature Superconductors." Cambridge Studies in Low

Temperature Physics. Cambridge: Cambridge University Press, 1999. doi:10.1017/CBO9780511524271.

[4] Economou, Eleftherios N. Green's functions in quantum physics. Vol. 3. New York: Springer, 1983.

[5] Hashimoto, Makoto, Inna M. Vishik, Rui-Hua He, Thomas P. Devereaux, and Zhi-Xun Shen. "Energy gaps in high-transition-temperature cuprate superconductors." Nature Physics 10, no. 7 (2014): 483-495.